AIP | Applied Physics Letters

Conduction band edge effective mass of La-doped BaSnO3

S. James Allen, Santosh Raghavan, Timo Schumann, Ka-Ming Law, and Susanne Stemmer

Citation: Applied Physics Letters **108**, 252107 (2016); doi: 10.1063/1.4954671
View online: http://dx.doi.org/10.1063/1.4954671
View Table of Contents: http://scitation.aip.org/content/aip/journal/apl/108/25?ver=pdfcov
Published by the AIP Publishing

Conduction band edge effective mass of La-doped $BaSnO_3$

S. James Allen,[1,a)] Santosh Raghavan,[2] Timo Schumann,[2] Ka-Ming Law,[1] and Susanne Stemmer[2]
[1]*Physics Department, University of California, Santa Barbara, California 93106-5100, USA*
[2]*Materials Department, University of California, Santa Barbara, California 93106-5050, USA*

(Received 25 April 2016; accepted 4 June 2016; published online 23 June 2016)

$BaSnO_3$ has attracted attention as a promising material for applications requiring wide band gap, high electron mobility semiconductors, and moreover possesses the same perovskite crystal structure as many functional oxides. A key parameter for these applications and for the interpretation of its properties is the conduction band effective mass. We measure the plasma frequency of La-doped $BaSnO_3$ thin films by glancing incidence, parallel-polarized resonant reflectivity. Using the known optical dielectric constant and measured electron density, the resonant frequency determines the band edge electron mass to be 0.19 ± 0.01. The results allow for testing band structure calculations and transport models. *Published by AIP Publishing*. [http://dx.doi.org/10.1063/1.4954671]

$BaSnO_3$ is a perovskite oxide that combines a wide band of ~3 eV (Refs. 1–3) with high electron mobilities and high carrier densities, which makes it of interest as transparent conductor, tunable plasmonic devices, and transistors that use the functional properties of perovskite oxides.[4] Room temperature mobilities as large as $\sim 300\,cm^2/V\,s$ have been reported in single crystals at carrier concentrations of $\sim 8 \times 10^{19}\,cm^{-3}$.[5,6] Mobilities of thin films grown by molecular beam epitaxy (MBE) reach $\sim 150\,cm^2/V\,s$.[7] The energy gap and electron mass are the key material parameters that determine the usefulness of $BaSnO_3$ for transparent electronics and plasmonics. Band structure calculations carried out by density functional theory have been used to determine the electron effective masses in $BaSnO_3$. Results vary from ~0.06 to $\sim 0.9\,m_e$,[2,8–12] where m_e is the free electron mass. Experimental measures of the electron mass are limited. Seo *et al.*[13] estimated the mass from a "plasma frequency" derived from the amplitude of the fitted Drude response and a Moss–Burstein shift that is consistent with an electron mass of $\sim 0.35\,m_e$. In contrast, the zero crossing frequency of the real dielectric function shown in Ref. 13 (the plasma frequency for the doped sample) combined with the undoped dielectric constant requires an effective mass of $\sim 0.65\,m_e$. Kim *et al.*[12] found a Moss–Burstein shift consistent with a mass of $0.6\,m_e$. A recent measure of the Moss–Burstein shift in $BaSnO_3$[14] is interpreted by assuming an electron mass of $\sim 0.22\,m_e$ derived from density functional theory,[10] but requires a renormalization of the band gap at high doping.

Here, we use glancing incidence parallel-polarized reflectivity from a thin epitaxial $BaSnO_3$ film to measure a resonant response at the plasma frequency.[15–17] This approach has two important features: (i) it is well suited to thin films; indeed it is only useful in the thin film limit and, (ii) it is a resonance technique and only requires measurement of the resonant frequency/identification of the plasma frequency. Using the known optical dielectric constant of $BaSnO_3$ and the measured electron density, the band edge electron mass is determined to be $\sim 0.19 \pm 0.01\,m_e$. The results clarify the experimental measurements, providing an anchor for band structure and transport models for $BaSnO_3$.

The reflectivity was measured on a 25 nm thick, epitaxial La-doped $BaSnO_3$ film grown by MBE on a (001) $SrTiO_3$ substrate. Details of the MBE approach and film microstructure characterization have been described elsewhere.[7] Room temperature Hall and resistivity measurements indicated a carrier density of $\sim 1.6 \times 10^{20}\,cm^{-3}$ and a mobility of $\sim 100\,cm^2/V\,s$, which is higher than other $BaSnO_3$ films on $SrTiO_3$ reported in the literature. $SrTiO_3$ has a large lattice mismatch with $BaSnO_3$ of more than 5%, which limits the achievable mobilities.[7] Compared with other films used for measurements of the effective mass in the literature[13] the films show a high degree of La donor activation. The lowest carrier concentration which could be measured was $1.6 \times 10^{19}\,cm^{-3}$,[7] which gives an upper limit for any trapped carriers of ~10% of the measured $1.6 \times 10^{20}\,cm^{-3}$.

Reflectivity was measured with a Bruker IFV/S Fourier transform spectrometer fitted with a Harrick Instruments AutoSeagull reflectometer and infrared polarizer. The angular acceptance of the reflected radiation was $\sim \pm 5°$. A computer controlled translation stage shuttled between a gold reference, a bare $SrTiO_3$ substrate, and the sample with the $BaSnO_3$ film. This enables accurate measurements of the differences in reflectivity between the bare substrate and the sample, especially at large angles where the plasmon resonance should emerge as the overall reflectivity becomes quite small near Brewster's angle.

Figure 1(a) shows a schematic of the electromagnetic waves that contribute to the parallel-polarized (p-polarized) reflectivity. Figure 1(b) shows the angle dependence of the p-polarized reflectivity of the sample referenced to gold. The structure below $1000\,cm^{-1}$ marks the beginning of the reststrahlen region and should be ignored. The resonant dip at $\sim 4000\,cm^{-1}$, which develops at large angle, is assigned to the plasma oscillations of the electron gas normal to the interface. Its frequency is related to the electron density, n, effective mass, m^*, and dielectric constant, ε, at the plasma frequency ω_p, by

a)Author to whom correspondence should be addressed. Electronic mail: allen@itst.ucsb.edu

$$\omega_p = \left(\frac{ne^2}{\varepsilon m^*}\right)^{1/2}, \tag{1}$$

where e is the electron charge. Using the electron density determined by the Hall effect and the dielectric constant (4.2) determined from measurements on single crystal $BaSnO_3$ (Ref. 18), we determine the m^* to be 0.19 ± 0.01. The uncertainty in the mass value is related to estimates of the uncertainty in the resonant position, ω_p, and uncertainty in the dielectric constant.[19] We assume that the uncertainty in the electron density is not significant here.

To support this straightforward identification of the resonant dip as the plasma oscillation of the electron gas, we used a quantitative electrodynamic model of the p-polarized plasma resonance of an optically thin film,[15–17] as described in the supplementary material,[19] and compare the result with the experiment. We emphasize that the purpose of this model is to gain confidence that the resonant position can be assigned to the plasma frequency of the doped film. In the last analysis, it is only the resonant position that we need in order to measure the mass using Eq. (1).

The field reflectivity can be expressed in terms of the angular dependent wave impedances for the vacuum, the film, and the substrate

$$Z_{z,\alpha} = \frac{e_{x,\alpha}}{h_{y,\alpha}} = \left(\frac{\mu_0}{\varepsilon_\alpha} - \frac{k_x^2}{\omega^2 \varepsilon_\alpha^2}\right)^{1/2}. \tag{2}$$

$Z_{z,\alpha}$ is the ratio of $e_{x,\alpha}$, the x-component of the electric field propagating in medium α and the y-component of the companion magnetic field, $h_{y,\alpha}$. ε_α is the dielectric constant, including the Drude response in the case of the film,[19] with $\alpha = 1$, 2, and 3, for vacuum, film, and substrate, respectively. μ_0 is the permeability of free space and ω is the frequency of the radiation in rad/s. k_x is the same in each of the media and at a given angle of incidence is the projection of the incident radiation wave vector on the plane of the sample. The reflectivity expressed as the ratio of the radiation magnetic fields is given by

$$r = \frac{h_r}{h_i} = \frac{(Z_{z,1} - Z_{z,2})}{(Z_{z,1} + Z_{z,2})} + \frac{4e^{i\varphi} Z_{z,1} Z_{z,2} (Z_{z,2} - Z_{z,3})}{(Z_{z,1} + Z_{z,2})^2 (Z_{z,2} + Z_{z,3}) \left(1 - \frac{e^{i\phi}(Z_{z,1} - Z_{z,2})(-Z_{z,2} + Z_{z,3})}{(Z_{z,1} + Z_{z,2})(Z_{z,2} + Z_{z,3})}\right)}, \tag{3}$$

where h_r and h_i are the reflected and incident magnetic fields. The phase factor, ϕ, is $2dk_{z,2}$ where d is the film thickness and $k_{z,2}$ is the wave vector in the film, normal to the interfaces. The power reflectivity is $R = |r|^2$. Here, ϕ is small, and one could develop an approximate result for very thin films that may expose the plasma resonance analytically, but Fig. 1(c) shows the results obtained from the full expression as given by Eq. (3).

The agreement between experiment and the electrodynamic model is satisfactory. Specifically, the overall predictions of the model are close enough to the measurements that we can confidently assign the resonant feature to the plasma resonance of the film. The overall experimental reflectivity is somewhat higher than the model calculation. This is especially so at large angles, which are close to the Brewster's angle for the substrate. It seems likely that the experiment has some contamination from s-polarized radiation. At large angles the s-polarized radiation rises just as the p-polarized reflectivity vanishes at Brewster's angle. Most important the s-polarized radiation *does not* couple to plasma oscillations normal to the film surface. Indeed, at near normal incidence there is little difference between s- and p-polarized response and the p-polarized reflectivity shown in Fig. 1(b) at 15° shows little evidence of the feature that appears at large angle. Interpretation of the resonant response as the plasma oscillation should not be compromised by the small quantitative differences in the overall reflectivity. The noise apparent in the data in Fig. 1(b) does not compromise our determination of a resonance response. The two vertical lines show that the resonance is located well inside that region.

The line broadening, $1500\,cm^{-1}$, invoked in the model calculation is not small. We note that carrier relaxation rates for free carriers in the perovskite oxides for frequencies above the optical phonon frequencies are typically of the order of $\sim 2000\,cm^{-1}$, which makes $1500\,cm^{-1}$ assumed here reasonable. Nonetheless we can use the model displayed in Fig. 1(c) to explore the effect of line broadening on the resonant position of the plasma feature. Figure 2 shows that there is little effect of the scattering rate on the resonant position. The strength of the resonant feature is consistent with a scattering rate of $\sim 1500\,cm^{-1}$.

To summarize, the agreement between the electrodynamic model and experiment is more than sufficient to allow confident interpretation of the resonant dip as the thin film plasma frequency. The conduction band edge mass value of 0.19 ± 0.01 measured by resonant plasmon absorption comes with a caveat. With $m^* \sim 0.19$, the Fermi energy at a carrier density of $1.6 \times 10^{20}\,cm^{-3}$ is $\sim 0.5\,eV$. The optical probe that we use to measure the plasmon resonance is $\sim 4000\,cm^{-1}$ or $\sim 0.5\,eV$. This means that the electrons that contribute to the optical conductivity or optical dielectric constant, which determines the plasma resonance, includes nearly all the electrons in the Fermi sea. In a perfectly parabolic conduction band, all the carriers would be described by a single m^*. Many band structure calculations indicate non-parabolicity, leading to $\sim 10\%$ increase in electron mass at this Fermi energy. Then the measured m^* is some weighted average of

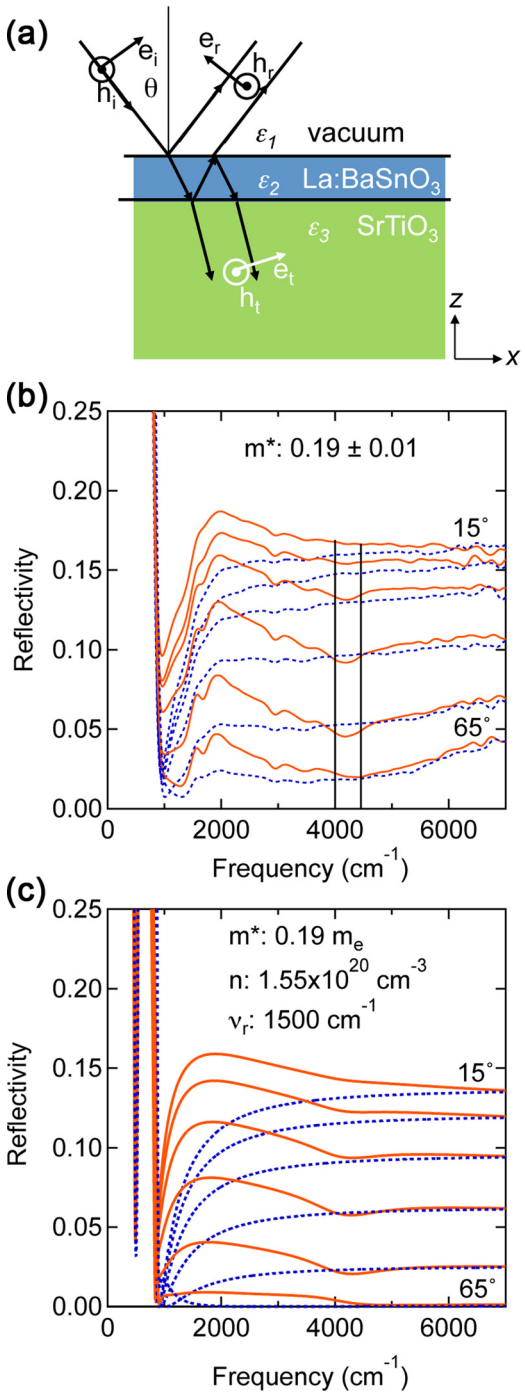

FIG. 1. (a) Schematic showing the transmitted electromagnetic waves that contribute to parallel polarized reflectivity and used in the electromagnetic model. (b) Measured frequency dependent reflectivity of a 25 nm thick film of La-doped $BaSnO_3$ on $SrTiO_3$ as a function of angle in increments of 10°. Vertical lines are to guide the eye to the resonant feature in the reflectivity. The blue dotted lines are the measured reflectivity of $SrTiO_3$ without $BaSnO_3$ layer. (c) Modeled frequency dependent reflectivity, using the parameters shown. As in (b), the blue dotted lines are calculated without the $BaSnO_3$ layer.

all the electrons in the Fermi sea. By this reasoning the measured m^* might be heavier than that at the very bottom of the conduction band. Thus, an m^* of 0.19 ± 0.01 represents an upper bound, and mass at the bottom of the conduction band could be ~10% smaller.

In conclusion, we have measured the resonant plasmon absorption in thin doped films of $BaSnO_3$ grown on $SrTiO_3$ by angular p-polarized reflectivity. With the aid of a well developed electrodynamic model of the reflectivity, which supports the picture of a well defined singular resonant response at the plasma frequency, we obtain an electron mass in $BaSnO_3$ that should provide a firm anchor for band structure calculations and transport models in this important transparent conducting oxide.

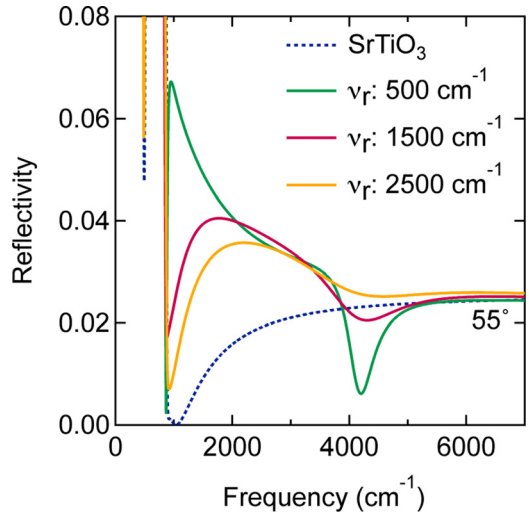

FIG. 2. The parallel polarized reflectivity at 55° modeled with three different Drude contributions corresponding to scattering rates of 2500, 1500, and 500 cm^{-1}.

S.J.A. acknowledges useful conversations with Karthik Krishnaswamy and Chris Van de Walle. The authors thank the Extreme Electron Concentration Devices (EXEDE) MURI of the Office of Naval Research (ONR) through Grant No. N00014-12-1-0976 for support of this work. Film growth experiments were supported by the U.S. National Science Foundation (Grant No. DMR-1409985).

[1]H. Mizoguchi, H. W. Eng, and P. M. Woodward, Inorg. Chem. **43**, 1667 (2004).
[2]S. Sallis, D. O. Scanlon, S. C. Chae, N. F. Quackenbush, D. A. Fischer, J. C. Woicik, J. H. Guo, S. W. Cheong, and L. F. J. Piper, Appl. Phys. Lett. **103**, 042105 (2013).
[3]S. A. Chambers, T. C. Kaspar, A. Prakash, G. Haugstad, and B. Jalan, Appl. Phys. Lett. **108**, 152104 (2016).
[4]S. Ismail-Beigi, F. J. Walker, S. W. Cheong, K. M. Rabe, and C. H. Ahn, APL Mater. **3**, 062510 (2015).
[5]H. J. Kim, U. Kim, H. M. Kim, T. H. Kim, H. S. Mun, B.-G. Jeon, K. T. Hong, W.-J. Lee, C. Ju, K. H. Kim *et al.*, Appl. Phys. Express **5**, 061102 (2012).
[6]X. Luo, Y. S. Oh, A. Sirenko, P. Gao, T. A. Tyson, K. Char, and S. W. Cheong, Appl. Phys. Lett. **100**, 172112 (2012).
[7]S. Raghavan, T. Schumann, H. Kim, J. Y. Zhang, T. A. Cain, and S. Stemmer, APL Mater. **4**, 016106 (2016).
[8]B. G. Kim, J. Y. Jo, and S. W. Cheong, J. Solid State Chem. **197**, 134 (2013).
[9]E. Moreira, J. M. Henriques, D. L. Azevedo, E. W. S. Caetano, V. N. Freire, and E. L. Albuquerque, J. Solid State Chem. **187**, 186 (2012).
[10]D. O. Scanlon, Phys. Rev. B **87**, 161201(R) (2013).
[11]H.-R. Liu, J.-H. Yang, H. J. Xiang, X. G. Gong, and S.-H. Wei, Appl. Phys. Lett. **102**, 112109 (2013).
[12]H. J. Kim, U. Kim, T. H. Kim, J. Kim, H. M. Kim, B. G. Jeon, W. J. Lee, H. S. Mun, K. T. Hong, J. Yu *et al.*, Phys. Rev. B **86**, 165205 (2012).
[13]D. Seo, K. Yu, Y. J. Chang, E. Sohn, K. H. Kim, and E. J. Choi, Appl. Phys. Lett. **104**, 022102 (2014).

[14]Z. Lebens-Higgins, D. O. Scanlon, H. Paik, S. Sallis, Y. Nie, M. Uchida, N. F. Quackenbush, M. J. Wahila, G. E. Sterbinsky, D. A. Arena *et al.*, Phys. Rev. Lett. **116**, 027602 (2016).
[15]R. A. Ferrell and E. A. Stern, Am. J. Phys. **30**, 810 (1962).
[16]B. Feuerbacher, R. P. Godwin, and M. Skibowski, Phys. Lett. A **26**, 595 (1968).
[17]D. W. Berreman, Phys. Rev. **130**, 2193 (1963).
[18]T. N. Stanislavchuk, A. A. Sirenko, A. P. Litvinchuk, X. Luo, and S. W. Cheong, J. Appl. Phys. **112**, 044108 (2012).
[19]See supplementary material at http://dx.doi.org/10.1063/1.4954671 for the reflectivity model used, a discussion of the dielectric constants used, and models of the plasmon resonances.